Sigma Journal of Engineering and Natural Sciences
Web page info: https://sigma.yildiz.edu.tr
DOI: 10.14744/sigma.2025.00106

Research Article

Impact of dust and wind on heat rejected from solar panel

Soud Ali SOUD[1,2,*], Dayang Radiah Awang BIAK[1], Mohamad Rezi Abdul HAMID[1], Shafreeza SOBRI[1]

[1]*Department of Chemical & Environmental Engineering, Faculty of Engineering, Universiti Putra Malaysia, Selangor, 43400, Malaysia*
[2]*Department of Chemical Engineering, Al-Muthanna University, Samawah, 66001, Iraq*

ARTICLE INFO

Article history
Received: 01 April 2024
Revised: 13 May 2024
Accepted: 30 August 2024

Keywords:
Dust Density; Heat Losses; Response Surface Methodology; Wind Direction; Wind Speed

ABSTRACT

A small portion of the solar energy is transformed into electric power. Residual energy has the potential to heat a solar cell which increases the temperature of the solar panel. An increase in heat rejection (losses) from the solar panel causes the phenomenon of urban heat islands (UHI); therefore, making heat losses at the lowest level of heat rejection to the environment is crucial. In this study, three factors were studied: dust density, wind speed, and wind direction. The methodology of response surface together with rotatable central composite design and full factorial method were utilised to create the work's experimental design, derive the mathematical model, and determine the ideal circumstances for the work that includes dust density of 1.145 g/m^2, wind velocity of 0.757 m/s, and wind direction two.

Cite this article as: Soud SA, Biak DRA, MRA Hamid, Sobri S. Impact of dust and wind on heat rejected from solar panel. Sigma J Eng Nat Sci 2025;43(4):1075−1087.

INTRODUCTION

As a result of the exhaustion of natural resources, such as crude oil and gas, the world is switching to renewable energy sources [1-3]. The importance of renewable energy sources, such as solar, wind, biomass, and hydropower, is increasing globally [4-6]. The arid region is an ideal location for constructing large photovoltaic power plants because it has an abundance of sun energy and inexpensive land resources [4]. However, extreme atmospheric conditions in these locations may have a negative effect on the ability of solar cells to generate electricity [6,7]. Rate of energy conversion of the commercially available PV technology typically ranges between five and twenty percent. Regrettably, this rate is reduced because the PV panel is constantly functioning at high temperatures. Typically, the efficiency degrades by 0.25%−0.5% for every degree Celsius [8,9].

Numerous studies have been conducted over the past decade to determine how different environmental conditions affect the performance of solar modules [9]. Additionally, the electrical competence of photovoltaic modules can be significantly affected by the operating temperature of the solar cells because of the characteristics of the crystalline silicone used in solar panels. The amount of energy that these cells produce decreases at high temperatures [10]. A large portion of solar radiation is converted into heat by photovoltaic cells, which has a negative effect on PV production [11].

***Corresponding author.**
*E-mail address: soudali2010@mu.edu.iq

This paper was recommended for publication in revised form by Editor-in-Chief Ahmet Selim Dalkilic

Published by Yıldız Technical University Press, İstanbul, Turkey

When the temperature of the surface module rises above a set threshold, the competence of the solar PV array dramatically declines [12]. The surface temperature of the PV panel rises quickly as solar radiation strikes it, which causes a sharp decline in the power output and PV panel efficiency [13,14]. Photovoltaic (PV) module performance decreases due to overheating, which is caused by a substantial amount of incoming solar radiation being transformed to heat [15-18].

Surface temperature and dust affect the effectiveness of conventional solar cells in generating electricity. The competence of PV power generation can be increased by lowering the surface temperature of solar cells and removing surface dust. The removal of dust and cooling have significant effects on the production of solar power, according to previous studies [18]. Xu et al. [4] studied how dust accumulation affected the temperature of the module. According to the results, under identical environmental conditions, the dust-deposited PV module temperature increased by approximately 64.7% in comparison to the clean PV module temperature.

Xu et al. [4] noticed that an increasing wind speed causes an exponential drop in the photovoltaic glass's final temperature. Vasel and Iakovidis [19] found that with all other effective elements remaining constant, the power output of the solar plant increased dramatically in the presence of a southerly breeze. Kaldellis et al. [20] found that when wind speed increases, the difference of temperature between the cell and the ambient temperature diminishes. Jha and Tripathy [21] discovered that a dusty panel's efficiency reduction on a windy sunny day was 19.5%. Mekhilef et al. [22] found more heat may be evacuated from the PV cell surface by increasing wind speed. Furthermore, wind spreads and lifts dust, which causes shadowing and subpar performance of the PV cells. Goverde et al. [23] investigated how wind speed affects an average decrease of the module's surface temperature. These procedures resulted in temperature drops of 11, 16, and 21 °C, with wind speeds of 1, 16, and 5 m s^{-1}, respectively. Goossens et al. [24] examined how soiling affected the wind's ability to cool and its implications for solar module performance. On a glass-glass module, cooling and electrical characteristics were assessed for wind velocities of up to four m/s, and soiling grades of up to forty-one g/m^2. Soiling can help photovoltaic modules cool down and the wind's impact on the module's performance.

EXPERIMENTAL SETUP

The trials were conducted at the Material Laboratory of the Engineering Faculty of the Universiti Putra Malaysia (UPM).

Apparatus

A sun simulator was used to obtain lighting. The simulated lighting system was constructed at the foundry laboratory of the engineering faculty. Solar irradiance obtained using LED lamps. Recent advancements in light-emitting diode (LED) lamps have made them a viable option for replicating solar radiation [25]. The light source system consists of three units of LED Flood Light lamps holding the trademark name Kontena, with a power output of 50 W each. The dimensions of the holder of the LED lamps were 1040 mm, 25 mm, and 500 mm with an equal distance of 100 mm between each bulb. The lamps were arranged in a single row.

Monocrystalline solar module with 36 solar cells. The technical specifications of the module are listed in Table 1. A monocrystalline solar module was positioned directly underneath the sun simulator at a distance of 380 mm, with both LED lamps and a solar panel tilted at 10° [26]. Temperature was measured using an infrared thermometer (RS-820) at one test point (on the centre of surface) of PV module with a resolution and accuracy of 0.1 °C and ± 1.0 °C, respectively.

An industrial fan (Mahita SF-650) at three speeds was used to generate wind velocities of 0 – 4 m/s. Additionally, an out-fan regulator was used to obtain accurate speeds. A handheld anemometer (Custom TL-300) was utilised to gauge the wind velocity and environmental temperature with resolution of 0.1 m s^{-1} and 0.1 °C, respectively.

Solar charge controller to protect the circuit. Battery to save the electrical power produced and then provide it to the load. The Photovoltaic inverter transforms DC power into AC energy. The load can be powered by DC or AC power. The rig of the experimental system is shown in Figure 1.

Preparation of the Dust

A sample of dust from the University of Putra Malaysia soil was collected. The concrete fragments and other large solids were manually removed. A sieve with a 0.6 mm opening was used to filter out larger particles. The sample was then heated in a furnace (Memmert UFB 400) at 105 °C for 24 h to ensure that it was dry and humidity-free. Subsequently, the sample was milled to obtain a homogeneous sample. This was accomplished using a Smooth Double Roll Crusher from the Premur Group. Subsequently, the sample was heated in a furnace (Memmert UFB 400) at 105 °C for 24 h to remove moisture.

Table 1. Technical characteristics of the photovoltaic module

Maxson solar panel	Model FNEF105-100
Maximum power (Pmax)	100 W
Voltage at Pmax	18 V
Current at Pmax (Imp)	5.56 A
Open - circuit voltage (Voc)	21.6 V
Short - circuit current (Isc)	6.12 A
Power tolerance	±3 W
Weight	7 Kg
Dimensions	1025 x 542 x 30 mm

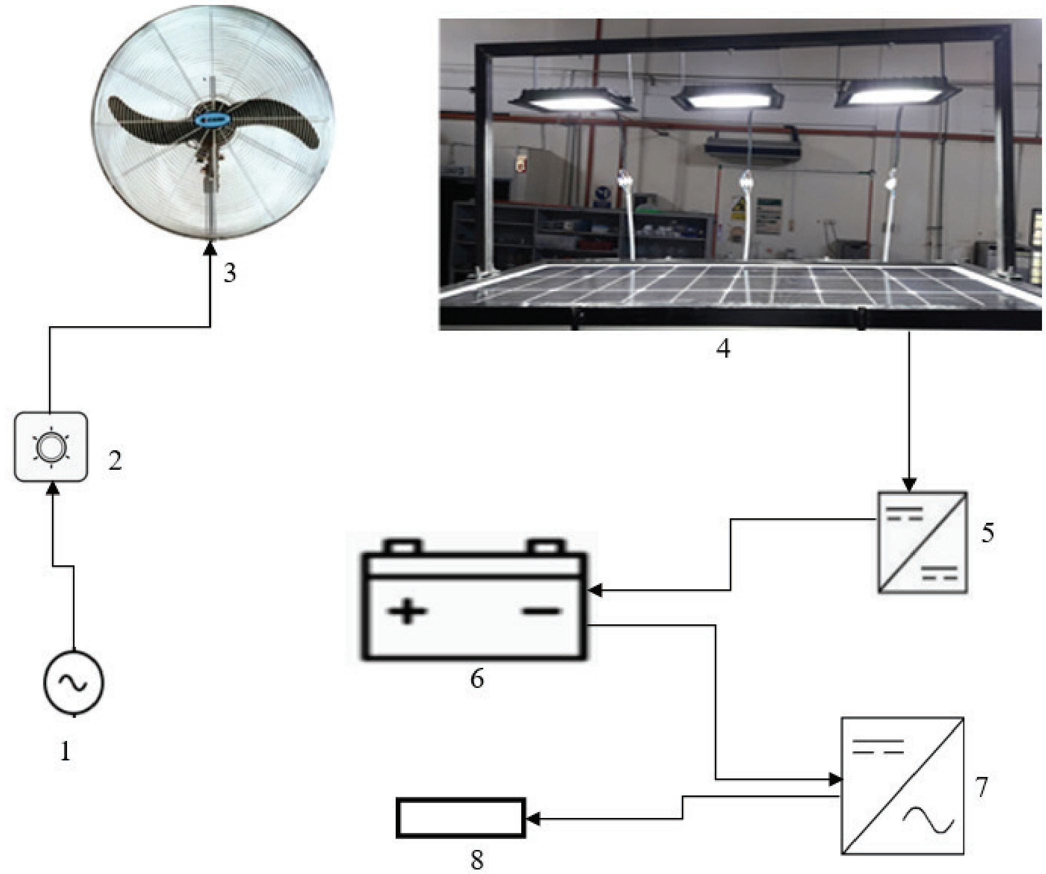

Figure 1. Experimental rig system (1) AC power, (2) Fan regulator, (3) Fan, (4) Solar panel with sun simulator, (5) Solar charge controller, (6) Battery, (7) Photovoltaic inverter, (8) Load.

Dust was added at various densities (0 - 8 g/m²). The dust was weighed using a balance (AND GF-300) with a maximum capacity of 310 g and a high precision of 0.0001. Every experiment in this study used a sieve with a 0.6 mm opening to spread the dust evenly. The solar panel was cleaned of dust at the end of each test run. The dust was then collected and disposed of.

EXPERIMENTAL DESIGN

A rotatable central composite design (CCD) with a full factorial method was utilized in order to plan the study's trials and create a mathematical model. This model describes the association between heat losses (response) together with the studied factors: dust density, wind speed, and wind direction. Minitab 19 was used as a tool.

A set of 26 experiments were conducted with base block one, ten cube centre points, 8 axial points, and 8 cube points. In which α = 1.41421 and a level of significance = 0.05. The independent factors (predictors) employed in this study were dust density (A), wind speed (B), and wind direction (C), while the dependent factor (response) was heat losses. The pace at which dust accumulates varies depending on the site environment. The dust densities at different places, periods, and seasons are shown in Table 2 [27]. Furthermore, the average wind velocity atlas in the

Table 2. Dust densities at different places, periods, and seasons

Country	Dust density g/m²	Period and season	Reference
Saudi Arabia	5	45 days	[30,31]
Pakistan	5.5	30 days	[29]
Indonesia	3.8	Dry	[31]
	1.7	rainy	
Iran	7.5	70 days	[32]

Table 3. Minimum and maximum values of input factors

Coded factor	Factor name	unit	Minimum value	Maximum value
A	dust density	g/m^2	0	8
B	wind speed	m/sec	0*	4
C	*wind direction	--	1 / 2**	1 / 2

* natural (free) stream (wind speed was 0.01 m/sec and was considered zero).

** wind direction: 1 in front of solar panel and 2 rear of solar panel.

Middle East at 10 m above ground is less than 4.5 m /s with the exception of a few places [25, 28,29]. For these reasons, in this study, the rate of dust density was 0 - 8 g/m^2, and the wind speed was 0 - 4 m/s. Table 3 displays the number of autonomous factors at minimum and maximum values.

The software (DOE) was used, and the results are listed in Table 4. Table 4 displays the factors without a response. Experiments were conducted, and the surface temperatures of the solar panel and air were recorded after 10 s for each run [4]. Each surface temperature represents the average of the five readings recorded. Furthermore, the solar panel

Table 4. The central composite design and heat losses values for the experiment

Std	Run	A	B	C*	Response
		Dust density	Wind speed	Wind direction	Heat losses
		g/m^2	m/sec	--	w/m^2
16	1	1.171	3.414	2	17.60
4	2	6.828	3.414	1	7.95
22	3	4.000	2.000	2	16.30
5	4	0.000	2.000	1	4.08
13	5	4.000	2.000	1	10.80
3	6	1.171	3.414	1	9.55
19	7	8.000	2.000	2	12.20
26	8	4.000	2.000	2	16.30
10	9	4.000	2.000	1	10.50
2	10	6.828	0.585	1	7.00
23	11	4.000	2.000	2	17.70
18	12	0.000	2.000	2	5.43
25	13	4.000	2.000	2	13.60
20	14	4.000	0.000	2	4.35
9	15	4.000	2.000	1	10.60
24	16	4.000	2.000	2	16.30
21	17	4.000	4.000	2	16.80
1	18	1.171	0.585	1	5.02
6	19	8.000	2.000	1	6.78
14	20	1.171	0.585	2	3.03
7	21	4.000	0.000	1	6.28
12	22	4.000	2.000	1	10.40
8	23	4.000	4.000	1	10.00
17	24	6.828	3.414	2	16.00
11	25	4.000	2.000	1	10.20
15	26	6.828	0.585	2	6.06

* Wind direction: 1 in front of solar panel and 2 back of solar panel.

was cooled and cleaned of dust for each run. Subsequently, the heat losses were calculated.

Heat losses include radiation and convection losses. It is the sum of the heat radiation loss and heat convection loss. Heat losses were calculated using equations (1-9) [33]. Radiation loss (Q_R) represents the heat exchanged between the glass layer of the PV panel and the environment, and can be computed in the manner described below:

$$Q_R = \varepsilon\,\sigma\,(T_s^4 - T_a^4) \tag{1}$$

The heat convection loss can be calculated using equation (2).

$$Q_C = h\,(T_s - T_a) \tag{2}$$

Local Nusselt number was used to find the value of the convective heat transfer coefficient. For forced convection: Nu = f (Re, Pr) while for free convection: Nu = f (Gr, Pr), where Nusselt, Reynold, Prandtl and Grashof numbers are dimensionless.

For forced convection:

$$Nu_x = 0.332\,Pr^{1/3}\;Re_x^{1/2} \tag{3}$$

Nu_x Indicate local values of the Nusselt number based on the fluid's characteristics and the distance from the leading edge of the plate.

$$\mathrm{Pr} = \frac{c_p\;\mu}{K} \tag{4}$$

$$Re_x = \frac{\rho\,u\,x}{\mu} \tag{5}$$

Re_x represents the local Reynolds number at any x position.

For free convection:

$$\mathrm{Nu} = \mathrm{C}(Gr\;Pr)^m \tag{6}$$

where the C and m values that are given for every case.

$$\mathrm{Gr} = \rho^2\,g\,\beta\,\Delta T\,x^3\,/\,\mu^2 \tag{7}$$

$$Nu_x = \frac{h_x\,x}{k} \tag{8}$$

$$h_x = Nu_x\,K\,/\,x \tag{9}$$

RESULTS AND DISCUSSION

Mathematical Model

The values of heat losses were recorded in table 4. Through experimentation and analysis using CCD technique, the quadratic model that predicts the connection between the heat losses and the independent variables utilised in this study was created using the values listed in table 4.

The outcomes indicate that the generated quadratic model is well-matched with the empirical data, with R^2 value 93.20 %, adjusted R^2 value 90.01 %, and a lack-of-fit p-value of 0.085. Equation 10 represents general (both directions). Equations 11 and 12 represent direction 1 and direction 2, respectively.

$$\text{Heat losses} = -4.07+3.726\,A+6.882\,B+1.355\,C1-1.355\,C2-0.3596A^2-0.880\,B^2-0.257A\,B-0.150\,A\,C1+0.150\,A\,C2-1.387\,B\,C1+1.387\,B\,C2 \tag{10}$$

$$\text{heat losses} = -2.72+3.576\,A+5.50\,B-0.3596\,A^2-0.880\,B^2-0.257AB \tag{11}$$

$$\text{heat losses} = -5.43+3.877\,A+8.27\,B-0.3596\,A^2-0.880\,B^2-0.257AB \tag{12}$$

Plotting predicted versus observed heat losses figures allows for additional confirmation of the model's correctness. The responses' residual plot values are displayed in Figures 2–6.

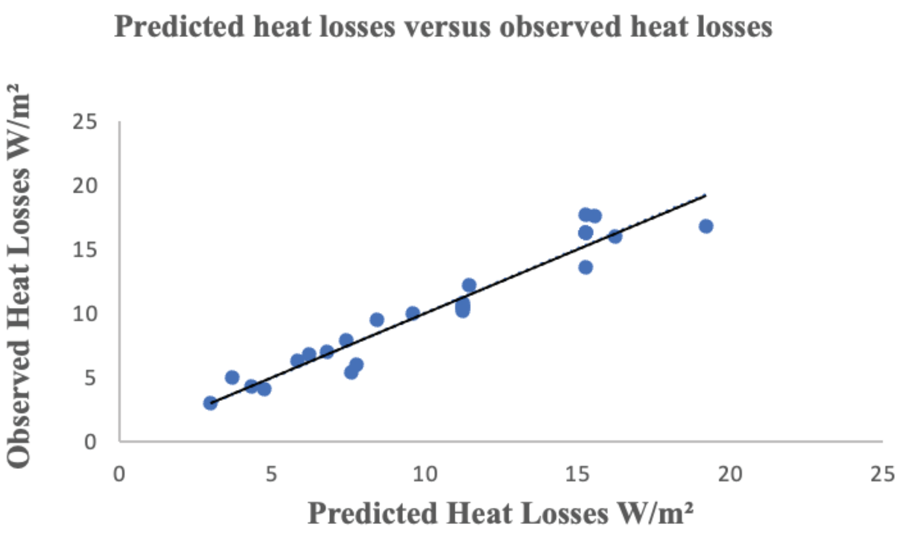

Figure 2. Predicted heat losses vs. observed heat losses

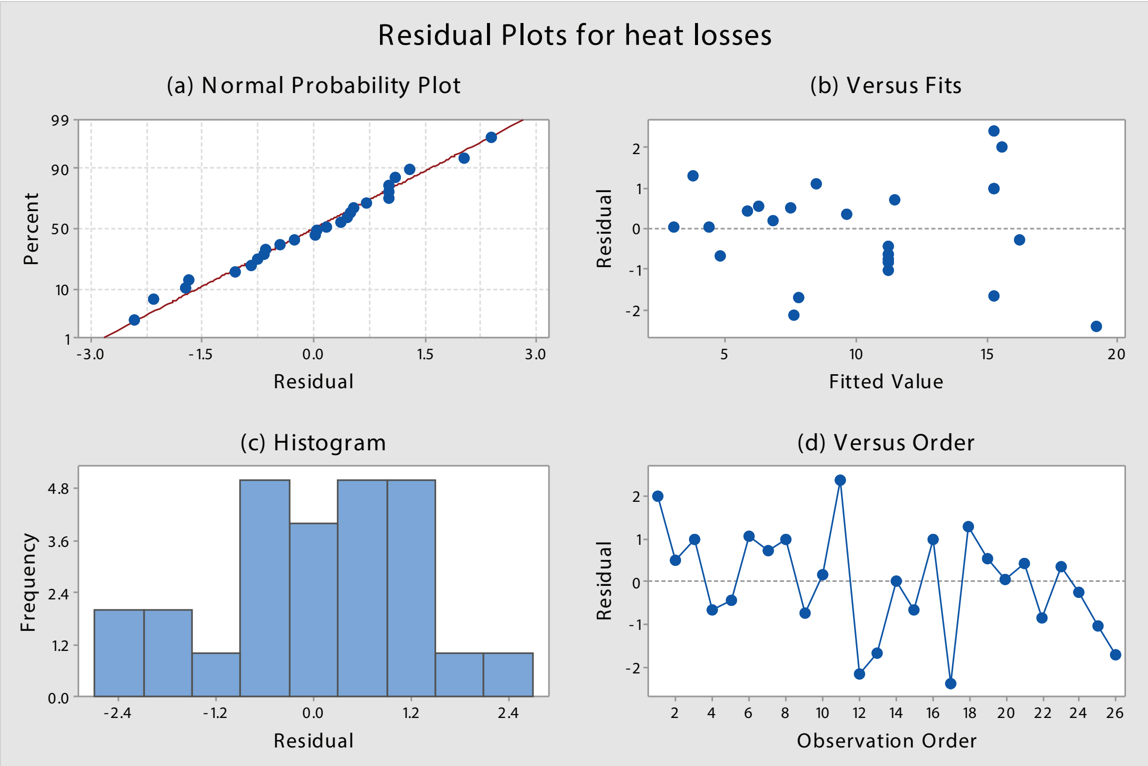

Figure 3. Residual plots for heat losses (a) normal probability, (b) versus fits, (c) histogram, and (d) observation order.

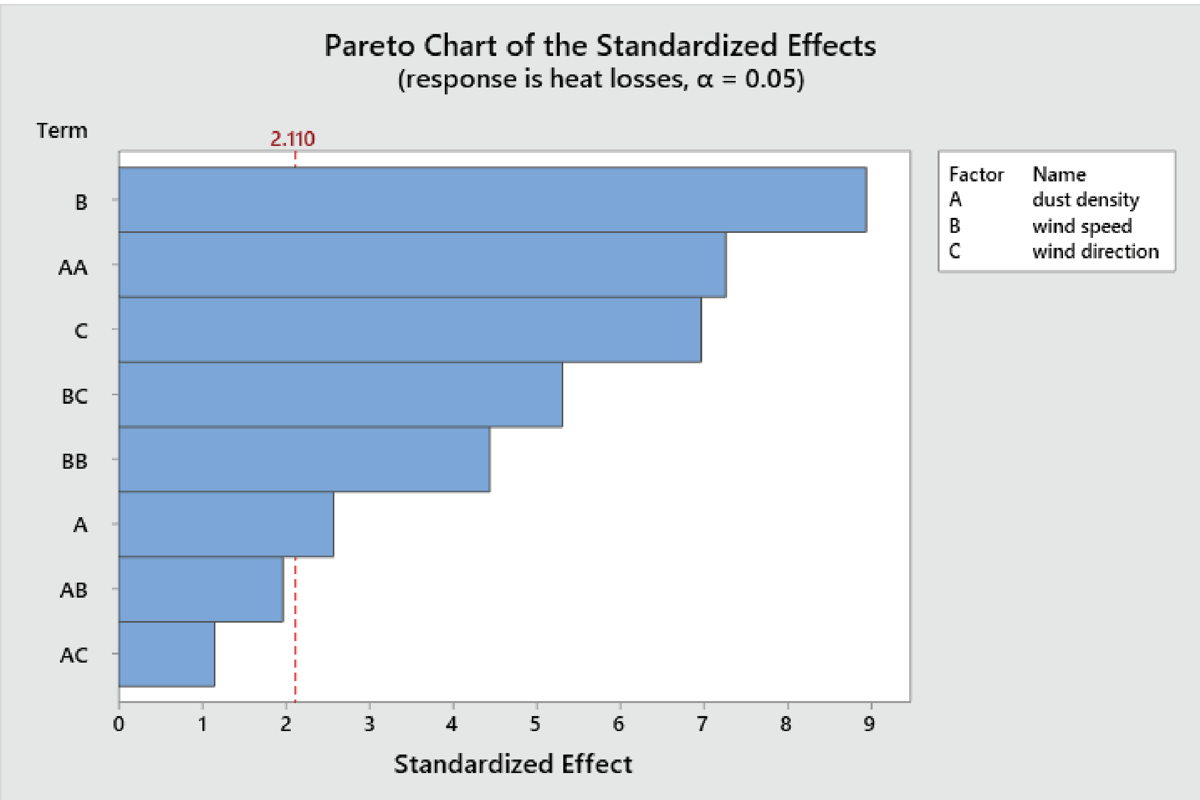

Figure 4. Pareto chart of the standardised effects.

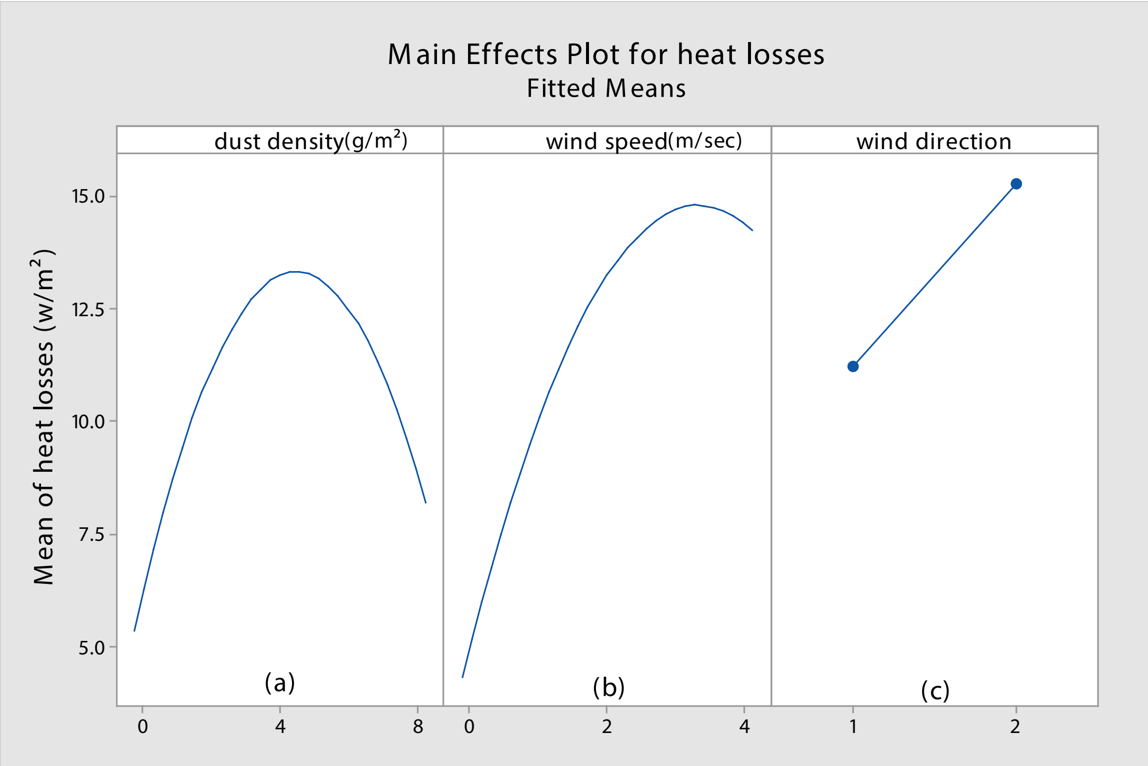

Figure 5. Main effects plot for heat losses: (a) effect of dust density, (b) effect of wind speed, and (c) effect of wind direction.

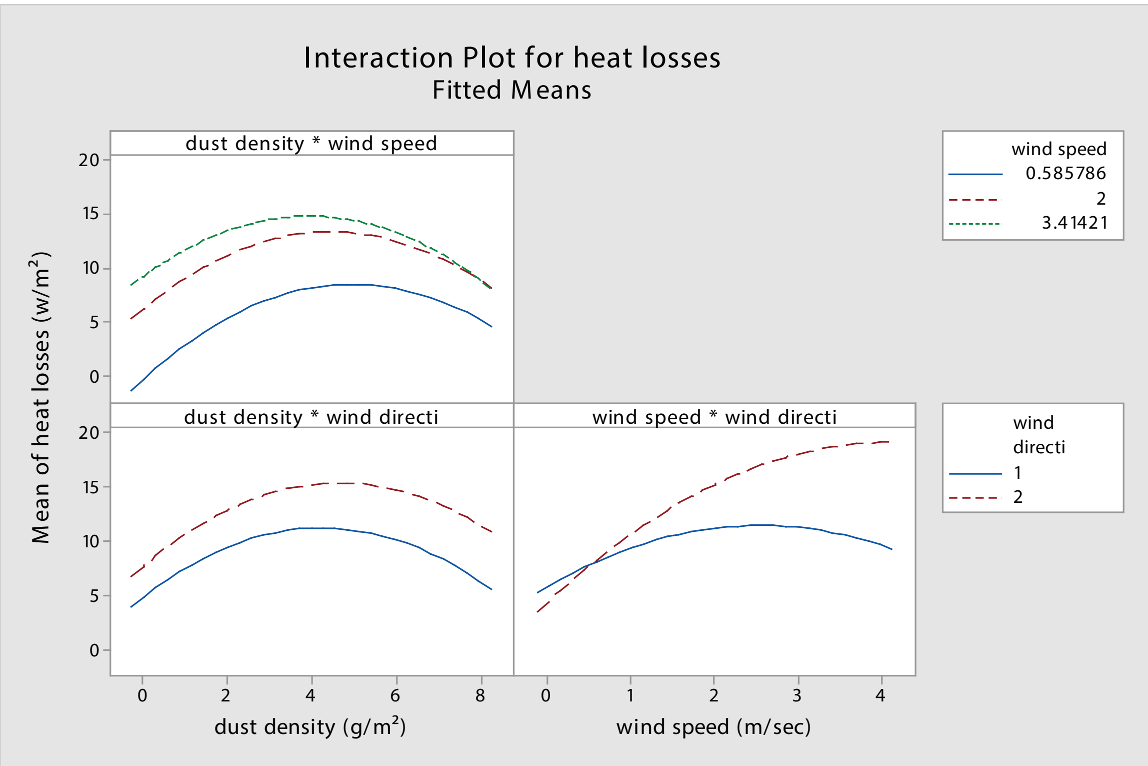

Figure 6. Interaction plot for heat losses.

The residual plot's normal probability is displayed in Figure 3a. In this figure, the points fall near the line. This suggests that the distribution of the data is normal and deviation from normality is small, therefore proving the projected model's accuracy.

The fit of the residual plot is disclosed in Figure 3b. The data shown in this figure is to be randomly distributed with no discernible pattern, suggesting that the variance is constant, and that validates the projected model's accuracy.

The residual vs. order plot is displayed in Figure 3d. It is possible to determine whether or not the variables are associated with one another from this plot. The data dispersion at random verifies that there is no correlation between the variables, indicating the accuracy of the projected model.

A Pareto chart can be used to show and compare the significance of each variable's standardised effect level on the heat losses (Fig. 4). It illustrates that the independent factors have a declining effect on the elimination percentage according to the order of: wind speed, wind direction, and dust density.

The influence of the investigated independent factors on the heat losses (response); are displayed in the main effects plot of these factors (Fig. 5). It demonstrated that heat losses increased as dust density rose within a given range. Any additional rise in dust density above that range, however, will have a detrimental effect on heat losses. Heat losses were increased when wind speed was increased to a particular range. Afterward, with each subsequent increase in wind speed, these losses decreased. In the wind direction, the heat losses in direction one is less than in direction two.

The links between the experimental variables and how they influence the response are shown in Figure 6.

Effect of Dust Density

The heat produced by the solar cells passes through the dust particles on the surface of module before exiting. A fraction of the heat is retained during this process because some of it is transmitted to the dust particles [24]. As shown in Figure 5a, positive effects of the dust density within the range of 0 - 4 g/m² on heat losses, due to the small quantity of dust particles on surface of module. At density above 4 g/m², the heat losses decreased because the dust particles absorbed a portion of this heat.

Effect of Wind Speed

As shown in Figure 5b, the heat losses increase with rising wind velocity from zero up to 3 m/s, due to the increasing variation in temperature between the solar panel's surface and the surrounding. At wind speed above 3 m/s the heat losses decreased because the temperature of PV glass dropped significantly as wind speed increased [4], which means reducing the temperature differential between the solar panel's surface and the surrounding.

Effect of Wind Direction

Figure 5c shows the heat losses at direction one was less than at direction two, due to the air blowing in front of the solar panel at direction one, which means reducing the variation in temperature between the solar panel's surface and its surroundings, while the air blowing in the rear of the solar panel at direction two and slight effect on temperature difference.

OPTIMISATION PROCESS

The response surface methodology is a statistical design that works effectively for data analysis and mathematical model prediction, whereas the CCD is a useful tool for optimising independent factors and getting the best possible response.

The relationships between variables and their influences on heat losses are demonstrated through surface and

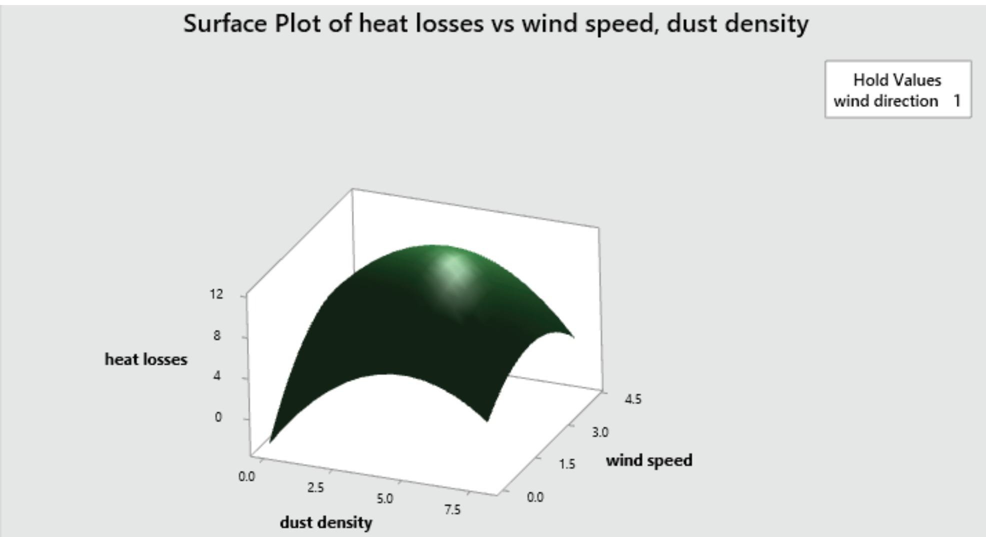

Figure 7. Surface plot of heat losses vs utilised variables for direction one.

contour plots of heat losses, as shown in Figures 7 and 8 for direction one, Figures 9 and 10 for direction two.

For direction one, Figure 8 illustrates that the region with 4.0 - 6.0 w/m² is the one with the best (lowest) heat losses. The zone limited by 0 - 5 w/m² for direction two is where the optimal (lowest) heat losses are found, as Figure 10 displays.

These figures were used to estimate the optimal conditions, and Table 5 ‘s parameters were used to carry out the optimisation method. Table 6 displays the optimal circumstances necessary to get the optimal response (minimum heat losses of 4.08).

In Figure 9, the optimisation plot of the minimum heat losses with the highest, lowest and optimal values for independent factors were presented.

In Figure 11, represented the minimal heat loss optimisation plot.

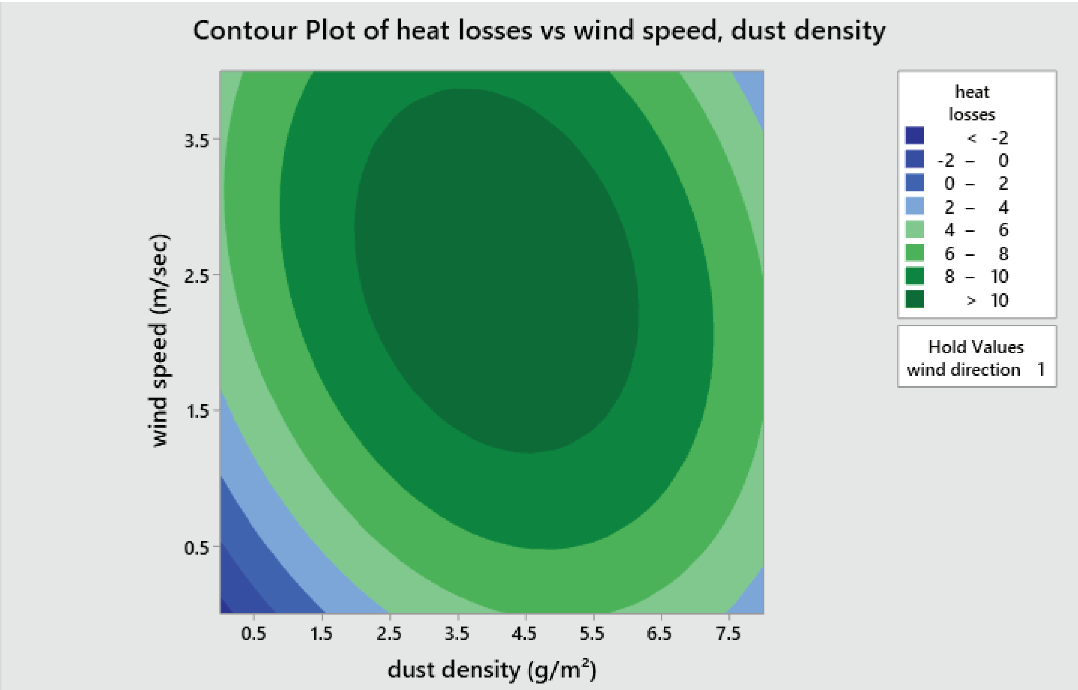

Figure 8. Contour plot of heat losses vs utilised variables for direction one.

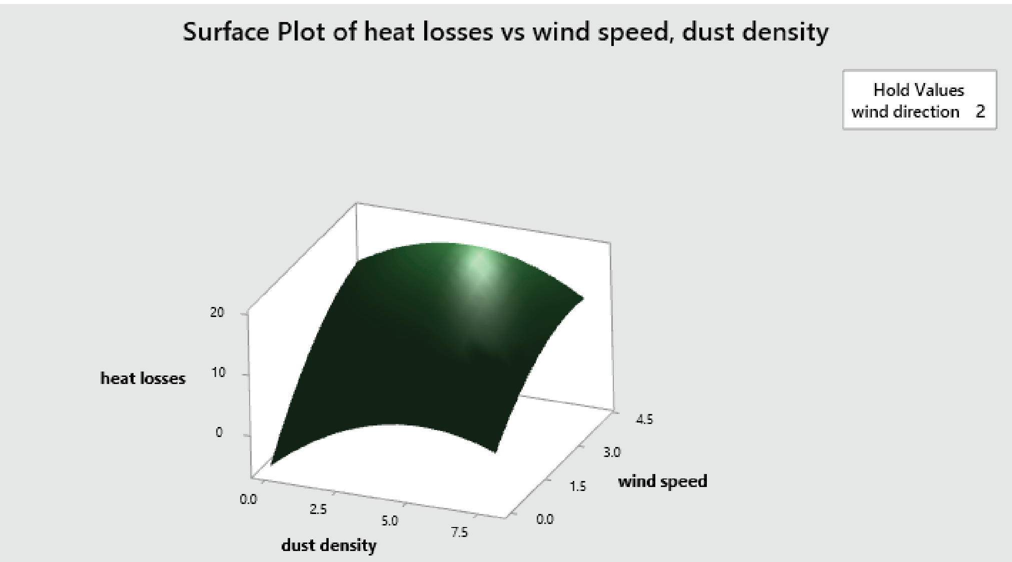

Figure 9. Surface plot of heat losses vs utilised variables for direction two.

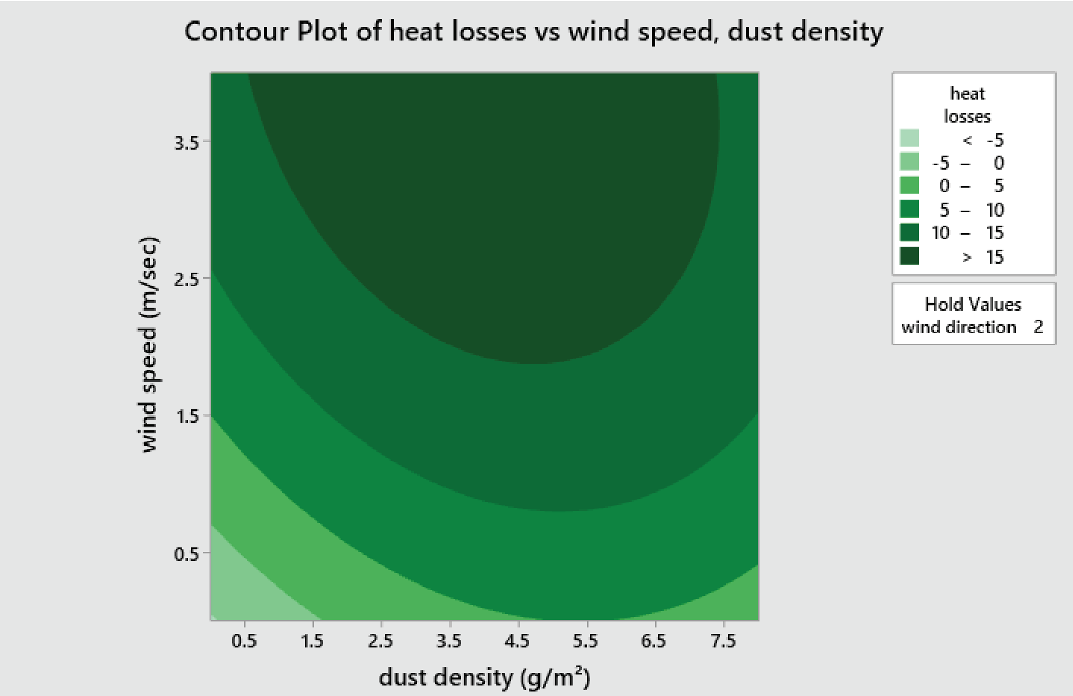

Figure 10. Contour plot of heat losses vs utilised variables for direction two.

Table 5. Parameter settings for optimisation

Response	Heat losses
Goal	target
lower	3.03
Target	4.08
Upper	17.7
weight	1
Importance	1

Table 6. Optimum conditions

Solution	1
Dust density	1.145
Wind speed	0.757
Wind direction	2
Heat losses fit	4.08
Composite desirability	1

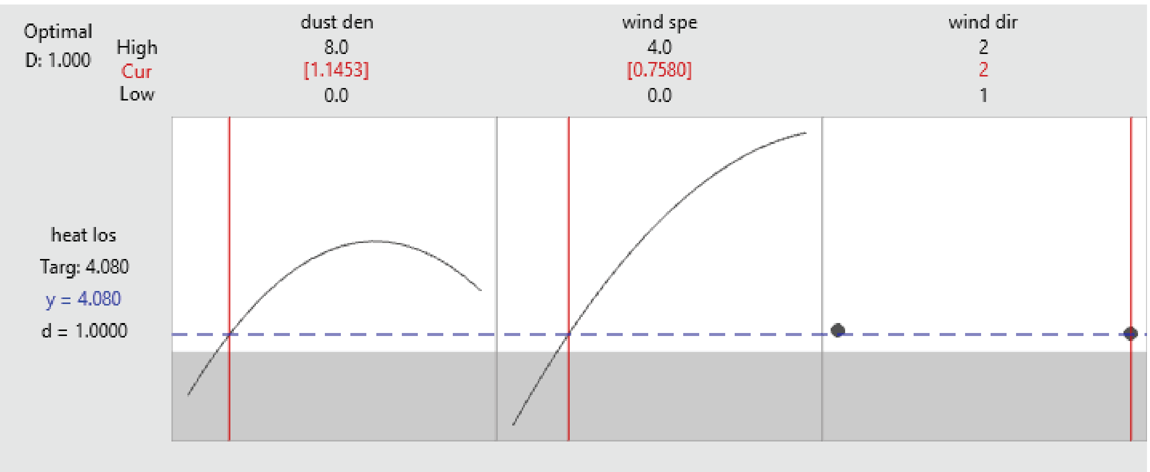

Figure 11. The minimal heat loss optimisation plot.

CONCLUSION

This study examined heat losses that were rejected from solar panels in two wind directions, and heat losses connected to the factors via full quadratic regression correlation. In addition, the optimal conditions were established and the impact of each individual variable on the response was examined. These were the conclusions reached:

- ❖ The mathematical pattern between heat losses and the factors was anticipated and its accuracy was tested using response surface methods and the central composite design for the experiments.
- ❖ Dust density positively impacts on heat losses within the range of 0 - 4 g/m^2, and negatively impacts on heat losses when it exceeds 4 g/m^2.
- ❖ The wind speed positively affects on heat losses within the range of 0 - 3 m/s, and when it exceeds 3 m/s there is a slight descent in heat losses.
- ❖ In general, the heat losses at direction one was lower than at direction two, due to the air blowing in front of the solar panel at direction one, while it was blowing in the rear for solar panel at direction two.
- ❖ The optimal conditions for the minimum heat losses were 1.145 g/m^2 of dust density and a wind velocity of 0.757 m s^{-1}, and wind direction two.

NOMENCLATURE

c_p	Specific heat (KJ/Kg °C)
g	acceleration of gravity (m/s^2)
Gr	Grashof number
h	Convective heat transfer coefficient (W/m^2 °C)
Imp	Current at Pmax (A)
Isc	Short circuit current (A)
k	Thermal conductivity (W/m °C)
Nu	Nusselt number
Nu_x	Local Nusselt number
Pmax	Maximum power (W)
Pr	Prandtl number
Q_C	Heat convection loss (W/m^2)
Q_R	Heat radiation loss (W/m^2)
Re	Reynold number
Re_x	Local Reynold number
Ta	Ambient temperature (°C)
Ts	Surface temperature (°C)
u	Velocity (m/s)
Voc	Open circuit voltage (V)
X	distance from ledge (m)

Greek symbols

B	Temperature coefficient (k^{-1})
μ	Viscosity (Kg/s m)
σ	Stefan Boltzmann constant 5.68x10^{-8} W/m^{2}K^4
ε	Emissivity of the glass
ρ	Density (kg/m^3)

Subscripts

a	Ambient
mp	Maximum power
oc	Open circuit
sc	Short circuit
s	Surface

Abbreviations

AC	Alternative current
C1	Direction 1
C2	Direction 2
CCD	Central composite design
DC	Direct current
DOE	Design of experiment
LED	Light emitting diode
PV	Photovoltaic module
UHI	Urban heat islands
UPM	Universiti Putra Malaysia

ACKNOWLEDGEMENTS

We would like to express our gratitude to the reviewers for their precise and succinct recommendations that improved the presentation of the results obtained.

AUTHORSHIP CONTRIBUTIONS

Authors equally contributed to this work.

DATA AVAILABILITY STATEMENT

The authors confirm that the data that supports the findings of this study are available within the article. Raw data that support the finding of this study are available from the corresponding author, upon reasonable request.

CONFLICT OF INTEREST

The author declared no potential conflicts of interest with respect to the research, authorship, and/or publication of this article.

ETHICS

There are no ethical issues with the publication of this manuscript.

REFERENCES

[1] Khalid HM, Rafique Z, Muyeen SM, Raqeeb A, Said Z, Saidur R, et al. Dust accumulation and aggregation on PV panels: An integrated survey on impacts, mathematical models, cleaning mechanisms, and possible sustainable solution. Sol Energy 2023;251:261–285. [CrossRef]

[2] Gielen D, Boshell F, Saygin D, Bazilian MD, Wagner N, Gorini R. The role of renewable energy in the global energy transformation. Energy Strateg Rev 2019;24:38–50. [CrossRef]

[3] Rashmi W, Mahesh V, Anirban S, Sharnil P, Khalid M. Hybrid solar PVT systems for thermal energy storage: Role of nanomaterials, challenges, and opportunities. Energy Syst Nanotechnol 2021;131–160. [CrossRef]

[4] Xu L, Li S, Jiang J, Liu T, Wu H, Wang J, et al. The influence of dust deposition on the temperature of soiling photovoltaic glass under lighting and windy conditions. Sol Energy 2020;199:491–496. [CrossRef]

[5] Kumar R, Singh SK. Solar photovoltaic modeling and simulation: As a renewable energy solution. Energy Rep 2018;4:701–712. [CrossRef]

[6] Al-Dousari A, Al-Nassar W, Al-Hemoud A, Alsaleh A, Ramadan A, Al-Dousari N, et al. Solar and wind energy: Challenges and solutions in desert regions. Energy 2019;176:184–194. [CrossRef]

[7] Koohestani SS, Nižetić S, Santamouris M. Comparative review and evaluation of state-of-the-art photovoltaic cooling technologies. J Clean Prod 2023;406:136953. [CrossRef]

[8] Hassan R, Aboaltabooq MHK. Photovoltaic panel cooling: A review of methodologies and technologies. Al-Furat J Innov Mech Sustain Energy Eng 2021;1:55–66. [CrossRef]

[9] Rabaia MKH, Abdelkareem MA, Sayed ET, Elsaid K, Chae KJ, Wilberforce T, et al. Environmental impacts of solar energy systems: A review. Sci Total Environ 2021;754:141989. [CrossRef]

[10] Hasan IA, Mohammed MJ, Attallah M. Analytical and experimental performance evaluation of direct flow cooling effect on PV panel. In: AIP Conference Proceedings. AIP Publishing; 2022. [CrossRef]

[11] Al-Jamea D, Masalha I, Alsabagh AS, Badran O, Maaitah H, Mashaqbeh O. Investigation on water immersing and spraying for cooling PV panel. Int Rev Mech Eng 2022;16:501–507. [CrossRef]

[12] Sunu PW, Anakottapary DS, Susila IDM, Triputra DGA, Indrayana NE, Asrori, et al. Preliminary study of solar PV characteristics cooled by water spray. In: Proceedings of the 4th International Conference on Applied Science and Technology on Engineering Science (iCAST-ES 2021). 2021. p. 429–433. [CrossRef]

[13] Naseer A, Jamil F, Ali HM, Ejaz A, Khushnood S, Ambreen T, et al. Role of phase change materials thickness for photovoltaic thermal management. Sustain Energy Technol Assess 2022;49:101719. [CrossRef]

[14] Alktranee M, Péter B. Energy and exergy analysis for photovoltaic modules cooled by evaporative cooling techniques. Energy Rep 2023;9:122–132. [CrossRef]

[15] Chanphavong L, Chanthaboune V, Phommachanh S, Vilaida X, Bounyanite P. Enhancement of performance and exergy analysis of a water-cooling solar photovoltaic panel. Total Environ Res Themes 2022;3:100018. [CrossRef]

[16] Sheik MS, Kakati P, Dandotiya D. A comprehensive review on various cooling techniques to decrease an operating temperature of solar photovoltaic panels. Energy Nexus 2022;8:100161. [CrossRef]

[17] Leow WZ, Irwan YM, Safwati I, Irwanto M, Amelia AR, Syafiqah Z, et al. Simulation study on photovoltaic panel temperature under different solar radiation using computational fluid dynamic method. J Phys Conf Ser 2020;1432:012052. [CrossRef]

[18] Li J, Xi Z, Wu S. Performance of autonomous temperature controlled photovoltaic modules with water film. IOP Conf Ser Earth Environ Sci 2019;267:032097. [CrossRef]

[19] Vasel A, Iakovidis F. The effect of wind direction on the performance of solar PV plants. Energy Convers Manag 2017;153:455–461. [CrossRef]

[20] Kaldellis JK, Kapsali M, Kavadias KA. Temperature and wind speed impact on the efficiency of PV installations. Experience obtained from outdoor measurements in Greece. Renew Energy 2014;66:612–624. [CrossRef]

[21] Jha A, Tripathy PP. Heat transfer modeling and performance evaluation of photovoltaic system in different seasonal and climatic conditions. Renew Energy 2019;135:856–865. [CrossRef]

[22] Mekhilef S, Saidur R, Kamalisarvestani M. Effect of dust, humidity and air velocity on efficiency of photovoltaic cells. Renew Sustain Energy Rev 2012;16:2920–2925. [CrossRef]

[23] Goverde H, Goossens D, Govaerts J, Dubey V, Catthoor F, Baert K, et al. Spatial and temporal analysis of wind effects on PV module temperature and performance. Sustain Energy Technol Assess 2015;11:36–41. [CrossRef]

[24] Goossens D, Lundholm R, Goverde H, Govaerts J. Effect of soiling on wind-induced cooling of photovoltaic modules and consequences for electrical performance. Sustain Energy Technol Assess 2019;34:116–125. [CrossRef]

[25] Hudisteanu SV, Chereches CN, Turcanu FE, Taranu N, Verdes M, Ancas AD, et al. Solar radiation simulation device for investigation of thermal and photovoltaic panels. Int J Mod Manuf Technol 2022;14:76–85. [CrossRef]

[26] Jacobson MZ, Jadhav V. World estimates of PV optimal tilt angles and ratios of sunlight incident upon tilted and tracked PV panels relative to horizontal panels. Solar Energy 2018;169:55–66. [CrossRef]

[27] Sakarapunthip N, Chenvidhya D, Chuangchote S, Chenvidhya T. Dust accumulation and its effect on PV performance in tropical climate and rice farm environment. In: 2021 IEEE 48th Photovoltaic Specialists Conference (PVSC); 2021; pp. 1848–1854. [CrossRef]

[28] Jahangiri M, Ghaderi R, Haghani A, Nematollahi O. Finding the best locations for establishment of

solar-wind power stations in Middle-East using GIS: A review. Renew Sustain Energy Rev 2016;66:38–52. [CrossRef]

[29] Ilse KK, Figgis BW, Werner M, Naumann V, Hagendorf C, Pöllmann H, et al. Comprehensive analysis of soiling and cementation processes on PV modules in Qatar. Sol Energy Mater Sol Cells 2018;186:309–323. [CrossRef]

[30] Said SA, Walwil HM. Fundamental studies on dust fouling effects on PV module performance. Sol Energy 2014;107:328–337. [CrossRef]

[31] Tanesab J, Parlevliet D, Whale J, Urmee T. Seasonal effect of dust on the degradation of PV modules performance deployed in different climate areas. Renew Energy 2017;111:105–115. [CrossRef]

[32] Gholami A, Saboonchi A, Alemrajabi AA. Experimental study of factors affecting dust accumulation and their effects on the transmission coefficient of glass for solar applications. Renew Energy 2017;112:466-473. [CrossRef]

[33] Holman JP. Heat transfer. 10th ed. New York: McGraw-Hill; 2010.